Articles

Cytosolic Half of Transmembrane Domain IV of the Human Bile Acid Transporter hASBT (SLC10A2) Forms Part of the Substrate Translocation Pathway[†]

Chandra M. Khantwal and Peter W. Swaan*

Department of Pharmaceutical Sciences, University of Maryland, 20 North Penn Street, Baltimore, Maryland 21201

Received December 20, 2007; Revised Manuscript Received January 31, 2008

ABSTRACT: We report the involvement of transmembrane domain 4 (TM4) of hASBT in forming the putative translocation pathway, using cysteine-scanning mutagenesis in conjunction with solvent-accessibility studies using the membrane-impermeant, sulfhydryl-specific methanethiosulfonate reagents. We individually mutated each of the 21 amino acids in TM4 to cysteine on a fully functional, MTS-resistant C270A−hASBT template. The single-cysteine mutants were expressed in COS-1 cells, and their cell surface expression levels, transport activities [uptake of the prototypical hASBT substrate taurocholic acid (TCA)], and sensitivities to MTS exposure were determined. Only P161 lacked cell-surface expression. Overall, cysteine replacement was tolerated at charged and polar residues, except for mutants I160C, Y162C, I165C, and G179C (≤20% TCA uptake versus the control). TCA uptake was significantly inhibited by MTSES and MTSET for N164C, T167C, S168C, A171C, V173C, and P175C. Interestingly, all of these residues were clustered along one face of the putative α helix. TM4 mutants were not sensitive to equilibrative (12 mM) sodium concentrations, thereby ruling out a direct role of TM4 in sodium translocation. Our results demonstrate that primarily the cytosolic half of TM4 is highly solvent-accessible and plays an important role in ASBT function and substrate translocation. Consistent with the existing experimental data, a three-dimensional model for the orientation of TM4 is proposed.

The apical sodium-dependent bile acid transporter (ASBT) and Na^+−taurocholate co-transporting protein (NTCP) are members of the solute carrier (SLC) 10A family, representing the major components in the active transport of bile acids across mammalian cell membranes. ASBT (SLC10A2) is a 39–41 kDa transmembrane glycoprotein, highly expressed in the ileocytes, cholangiocytes, and the kidney (*1–3*), and plays a pivotal role in maintaining the bile acid pool through enterohepatic circulation (*4–8*). Transport of bile acids by ASBT is facilitated by sodium symport in an electrogenic process with a 2:1 Na^+/bile acid stoichiometry (*9*). Inherited mutations in human ASBT (hASBT)[1] result in primary bile acid malabsorption syndrome (PBAM), suggesting that hASBT is the primary mechanism for intestinal reabsorption of bile acids (*6*). hASBT has seven transmembrane helices as confirmed by glycosylation and epitope insertion scanning mutagenesis (*10, 11*).

Expression of hASBT is under the control of hepatocyte nuclear factor HNF1α and is also regulated by bile acids through activation of nuclear farnesoid X receptor (FXR) using a negative-feedback control (*12–14*). Accordingly, interruption of the enterohepatic circulation of bile acids by inhibiting intestinal bile acid reabsorption via ASBT has been employed as a viable approach for cholesterol-lowering therapy (*15*). The decrease in bile acid reabsorption upregulates bile acid synthesis by hepatic cholesterol 7α-hydroxylase (*16*), thereby effectively reducing plasma cholesterol levels (*17–20*). Owing to its molecular promiscuity, hASBT is a viable intestinal prodrug target (*21*); for example, conjugation of the drug acyclovir to a bile acid using a valine linker resulted in a 2-fold enhancement in acyclovir bioavailability (*22*). Despite the pharmacological significance of hASBT, there is limited structural information available, thus hampering the rational design of drugs and prodrugs as substrates. Our laboratory has taken a systematic approach using a combination of computational techniques and molecular biology to unravel protein–substrate and protein−cation interactions to further define their binding and translocation mechanisms. Using a homology model to determine putative ligand-binding domains, we found that transmembrane domains 3, 4, 6, and 7 were likely candidates for substrate−TM interactions. Indeed, we recently demonstrated that transmembrane domain (TM) 7 forms an amphipathic α helix, which forms part of the bile acid permeation pathway (*23*).

[†] This work was supported by the National Institutes of Health (NIH) Grant DK061425 (to P.W.S.).

* To whom correspondence should be addressed: Department of Pharmaceutical Sciences University of Maryland, 20 Penn Street, Baltimore, Maryland 21201. Telephone: 410-706-0103. Fax: 410-706-5017. E-mail: pswaan@rx.umaryland.edu.

[1] Abbreviations: TM4, transmembrane (domain) 4; MTSES, sodium (2-sulfonatoethyl)methanethiosulfonate; MTSET, [2-(trimethylammonium)ethyl]methanethiosulfonate bromide; GDCA, glycodeoxycholic acid; hASBT, human apical sodium-dependent bile acid transporter; Ntcp, sodium taurocholate co-transporting polypeptide; TCA, taurocholic acid.

10.1021/bi702498w CCC: $40.75
Published on Web 03/01/2008

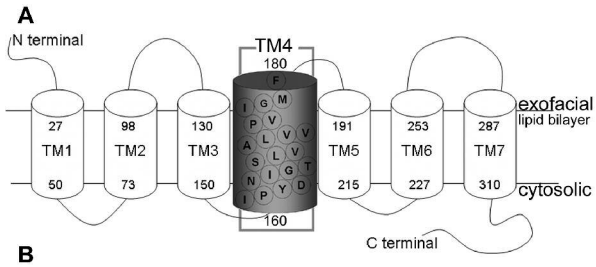

B

```
Human        160 IPYDNIGTSLVALVVPVSIGM
Rat          160 IPYDSIGISLVALVIPVSIGM
Mouse        160 IPYDSIGISLVALVIPVSFGM
Rabbit       161 IPYDNIGTSLVALVVPVSIGM
Hamster      160 IPYDSIGTSLVALVIPVSIGM
Dog          160 IPFDNIGTSLVALVVPVSIGM

Orangutan    171 IPYDNIGTSLVALVVPVSIGM
Chimpanzee   333 IPYDNIGTSLVALVVPVSIGM
Chicken      170 LPYDSIGISLVALVVPVSVGV
Cow          183 IPYDNIGISLVALVVPVSLGM
Zebrafish    161 IPYDNIGITLVSLLVPVGLGM
Pufferfish   131 IPFDSIGITLVALLVPIALGM
                 :*:*.** :**:*::*:..*:
```

FIGURE 1: Secondary-structure model of hASBT, residues of TM4, and protein sequence alignment of TM4 of ASBT from different species. (A) hASBT topology model with putative α-helical arrangement of TM4 residues 160–180 within the plasma membrane in net projection. (B) ClustalW alignment of 12 members of the SLC10A2 family, indicating conserved amino acid residues. The top group demonstrates the protein alignment of species commonly used in pharmacological testing, whereas the lower group denotes additional eukaryotic species. An asterisk (∗) indicates a strongly charged group; a colon (:) signifies a single fully conserved residue; and a period (.) indicates a weakly conserved group.

In the same study, hydroxyl-containing amino acid side chains within TM7 were suggested to form the bile acid binding site(s) via hydrogen-bond formation with bile acid hydroxyl groups.

In the present study, we used the substituted cysteine accessibility method (SCAM) to examine the possible role of TM4 in the formation of the hASBT substrate translocation pathway. TM4 is an appealing target for the following reasons: (1) TM4 contains one of the most conserved protein sequences within SLC10A2 with high sequence identity and homology (>90%) among a large number of species, ranging from human to fish (Figure 1); (2) TM4 contains a negatively charged residue along with five polar residues that can potentially be involved in hydrogen-bonding interactions; (3) helix projections of TM4 yielded a distinct polar face of the helix that may be solvent-accessible (Figure 1); (4) Ala mutants of V160, L163, and V166 in SLC10A1 (corresponds to G166, L169, and L172 in SLC10A2) exhibited markedly reduced TCA uptake, suggesting a highly ordered secondary structure (*24*); (5) TM4 contains an functionally silent, inherited mutation (A171S) with a 28% population frequency (*25*). Thus, TM4 constitutes an attractive target that may reveal valuable insight into ASBT function. Indeed, our data indicate that TM4 is a relatively solvent-accessible transmembrane helix with a cytoplasmic half that poorly tolerates cysteine mutations, suggesting their importance in hASBT structure and function.

EXPERIMENTAL PROCEDURES

Materials. [^{3}H]-Taurocholic acid (50 Ci/mmol) (TCA) was purchased from American Radiolabeled Chemicals, Inc. (St. Louis, MO); MTS reagents MTSES and MTSET were purchased from Toronto Research Chemicals, Inc. (North York, Ontario, Canada); sulfo-NHS-LC biotin was purchased from Pierce Biotech (Rockford, IL); and taurocholic acid and glychodeoxycholic acid (GDCA) were purchased from Sigma (St. Louis, MO). Cell-culture media and supplies were obtained from Invitrogen (Carlsbad, CA). All other reagents and chemicals were of highest purity available commercially.

Cell Culture. The monkey kidney fibroblast cell line, COS-1 (CRL-1650), was obtained from American Type Culture Collection (ATCC; Manassas, VA). Cells were grown and maintained in Dulbecco's modified Eagle's medium supplemented with 10% fetal bovine serum, with high glucose, and penicillin and streptomycin (Invitrogen) at 37 °C in a humidified atmosphere with 5% CO_2.

Site-Directed Mutagenesis and Transient Transfection. The pCMV vector containing cDNA of the hASBT−C270A construct was used to incorporate site-directed mutations using the Quick Change site-directed mutagenesis kit from Stratagene (La Jolla, CA), according to instructions of the manufacturer. Mutagenesis primers integrating cysteine substitutions of each individual residue in TM4 were custom-synthesized and purchased from Sigma Genosys (St. Louis, MO). Plasmid purification was accomplished using a kit from Qiagen (Valencia, CA) with verification of amino acid replacement for all mutants performed by DNA sequencing using a 3700 DNA analyzer (Applied Biosystems, Foster City, CA) at the Plant-Microbe Genomics Facility of The Ohio State University. Transient transfections in COS-1 cells were performed using the Lipofectamine Plus reagent (Invitrogen) and after 48 h processed for [^{3}H]-TCA uptake, Western blot analysis, and cell-surface biotinylation. α-Integrin, an integral plasma membrane protein, was used as a positive control in all immunoassays. The specificity of the biotinylation reaction was verified by the fact that no band could be detected when COS-1 cells transfected with wt-hASBT, and mutants were subjected to all labeling steps in the absence of sulfo-NHS-LC biotin. To ensure that the biotinylation agent did not have access to the intracellular environment because of membrane disruption, additional immunoblotting for the abundant ER protein calnexin was performed using a specific anticalnexin monoclonal antibody; as expected, upon biotinylation, no bands for calnexin were detected (data not shown).

Uptake Assay and Inhibition Studies. Cells transfected with native hASBT and mutant plasmids were used 48 h post-transfection to determine the uptake activity. Initial rates of ligand uptake were determined in transfected COS-1 cells incubated in modified Hanks' balanced salt solution (MHBSS) at pH 7.4 uptake buffer containing 5.0 μM [^{3}H]-TCA at 37 °C for 12 min. We have previously determined that this uptake period ensures linear steady-state kinetics in conjunction with an optimal signal-to-noise ratio for subsequent [^{3}H]-TCA analysis via liquid scintillation counting (*10, 23, 26*). Uptake was halted by a series of washes with ice-cold DPBS at pH 7.4 containing 0.2% fatty acid free bovine serum albumin (BSA) and 0.5 mM TCA. Cells were lysed in 350 μL of 1 N NaOH and subjected to liquid scintillation counting using a LS6500 liquid scintillation counter (Beckmann Coulter, Inc., Fullerton, CA) and total protein quantification using the Bradford protein assay (Bio-

Rad, Hercules, CA). Uptake activity was calculated as picomoles of [^{3}H]-TCA internalized per minute per milligram of protein.

MTS Inhibition Studies. Sensitivity of mutants to charged, membrane-impermeant MTS reagents was assessed by pretreatment of transiently transfected COS-1 cells with either 1.0 mM MTSES or MTSET for 10 min at room temperature. After MTS treatment, cells were washed twice in DPBS (Sigma, St. Louis, MO) and [^{3}H]-TCA uptake was measured as described above. Because of the short aqueous half-life of these MTS reagents, all solutions were freshly prepared prior to each study. Untreated controls with buffer in the absence of MTS reagents were run in parallel. Cell viability was determined using the live/dead assay (Molecular Probes, Inc., Eugene, OR) as per instructions of the manufacturer.

Sodium Activation Assay. Determination of [^{3}H]-TCA uptake in the presence of 12 mM [Na^+], reflecting an equilibrative [Na^+] resulting in no net inward Na^+ flux, was conducted for each mutant (uptake conducted as described above; choline chloride used as equimolar NaCl replacement) to assess the degree of Na^+ sensitivity for each mutant transporter. The ratio of TCA uptake at 12 mM versus 137 mM [Na^+] was calculated for each mutant. Typically, Na^+ ratios equal to 1 signify little measurable effect of extracellular [Na^+] on transport activity, while fractions less than 1 imply greater necessity for physiological [Na^+] to ensure proper function of a mutant transporter.

Substrate Protection Assay. The effect of substrates on MTSES/MTSET labeling was determined in transfected COS-1. Cells were washed twice in 1× phosphate-buffered saline (PBS) at pH 7.4 followed by incubation with GDCA (0–200 μM) for 3 min at room temperature followed by co-incubation with 1.0 mM MTSET or MTSET for 5 min (*27*). After pre-incubation treatments, cells were washed twice in MHBSS at pH 7.4 and additionally equilibrated for 15 min at 37 °C in this buffer followed by determination of 5 μM [^{3}H]-TCA uptake as described above. All control wells were treated identically.

Computational Analysis. Solvent accessibility within hASBT and regions around TM4 was calculated using a previously developed three-dimensional model for hASBT (*11*). The SiteID subroutine within the SYBYL software suite (version 6.9; Tripos Associates, St. Louis, MO) was employed to determine binding pockets. Local clefts are detected in SiteID by an atom-based solvent-accessibility method. The Grid algorithm was used to detect deep pockets and cavities within the hASBT protein. The grid was specified using a 1.0 Å resolution and 2.0 Å protein film depth. All other parameters were set to default values, except for the minimum population of grid points in a cluster, which was set to 15. The inner core of the protein was rendered accessible to the solvent from both the extra- and intracellular environment. Thus, the results represent the total solvent accessibility, and only clusters pertaining to TM4 are shown in Figure 7. Images were rendered within the biopolymer module within SYBYL.

Statistical Analysis. Uptake and MTS reagent inhibition data were analyzed for statistical significance using the two-tailed, unpaired Student's *t* test or one-way analysis of variation (ANOVA) with Dunnett's posthoc test; data were considered statistically significant at $p \leq 0.05$.

Table 1: Cysteine-Scanning Mutagenesis of TM4[a]

residue number	amino acid change	codon change
160	Ile → Cys	ATT → TGC
161	Pro → Cys	CCC → TGC
162	Phe → Cys	TAT → TGC
163	Asp → Cys	GAT → TGC
164	Asn → Cys	AAC → TGC
165	Ile → Cys	ATA → TGC
166	Gly → Cys	GGT → TGT
167	Thr → Cys	ACA → TGC
168	Ser → Cys	TCT → TGC
169	Leu → Cys	CTG → TGC
170	Val → Cys	GTT → TGC
171	Ala → Cys	GCT → TGC
172	Leu → Cys	CTC → TGC
173	Val → Cys	GTT → TGC
174	Val → Cys	GTT → TGC
175	Pro → Cys	CCT → TGC
176	Val → Cys	GTT → TGT
177	Ser → Cys	TCC → TGC
178	Ile → Cys	ATT → TGT
179	Gly → Cys	GGA → TGC
180	Met → Cys	ATG → TGC

[a] cDNA encoding cysteine-scanning scaffold C270A of hASBT was subjected to site-directed mutagenesis with cysteine replacements. Residue numbers in the table refer to the amino acid numbering for hASBT.

RESULTS

An alignment of amino acid residues 160–180 of the human ASBT sequence with 11 known orthologues demonstrates its high conservation with 17 of 21 residues maintaining identity or strong sequence similarity among a range of evolutionarily diverse species (Figure 1B). In this study, we used the hASBT mutant encoding a cysteine-scanning scaffold, in which a MTS-sensitive cysteine at position 270 was changed to alanine. This scanning scaffold exhibits transport activity similar to wild-type hASBT (*26*) and was used to construct cysteine mutants for each individual TM4 residue (Table 1).

To define the potential effects of point mutations on the cellular distribution of C270A mutants, they were transiently transfected into COS-1 cells. The membrane distributions of these mutants were confirmed by plasma membrane biotinylation, immunoblotting, and densitometric analysis of the developed bands (Figure 2). Individual cysteine mutants were expressed at varying concentrations in COS-1 cells necessitating normalization of the uptake data to protein expression levels, allowing us to directly compare the uptake activities of the mutants with the C270A transporter scaffold (control) (Figure 3). Cell-surface expression was observed for 20 of the 21 mutants, with the exception of P161C, which faces the cytosolic part of the TM4. This mutant was expressed at levels below detection limits both at the plasma membrane as well as in whole-cell lysate preparations (data not shown), suggesting that the mutation may alter protein stability, folding, or synthesis. Conversely, we hypothesized that altered transport activity of the cell-surface-expressed mutants could not be ascribed to synthesis or trafficking defects but simply reflect mutation-induced changes in hASBT affinity for its substrate, taurocholic acid.

The relative transport activity of each mutant, as measured by [^{3}H]-TCA uptake, was normalized to whole-cell protein expression as well as cell-surface expression (densitometric analysis) (Figure 3) to account for variability in transfection efficiency in COS-1 cells. In addition to the dysfunctional

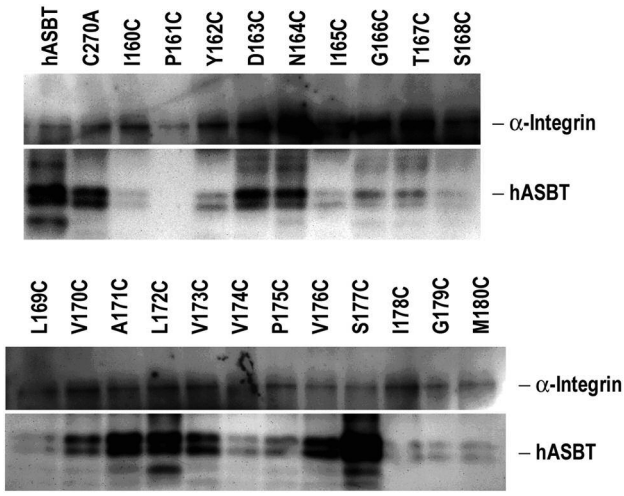

FIGURE 2: Expression of TM4 C270A mutants in COS-1 cells. Cell-surface biotinylation and Western blot analysis of these transporters were performed by transfecting COS-1 cells with the individual mutants. At 48 h post-transfection, the COS-1 cells were biotinylated with sulfo-NHS-LC biotin for 30 min at room temperature. Immunoprecipitation was carried out followed by Western blot analysis using affinity-purified rabbit anti-hASBT antibody and was visualized using goat antirabbit horseradish peroxidase (HRP)-conjugated secondary antibody. Glycosylated (top) and unglycosylated (bottom) bands of hASBT were detected in the biotinylated samples. Lysates were also probed with anti-α-integrin (150 kDa) antibody to allow semiquantitative analysis of hASBT band density.

mutant P161C, amino acid substitution at I160C, Y162C, I165C, and G179C resulted in minimal (≤20%) functional activity. Furthermore, mutants N164C, L169C, L172C, V176C, and M180C showed a significant reduction (≤80%) in [^{3}H]-TCA uptake. Overall, the effects of cysteine substitutions within the cytosolic half of TM4 were relatively more pronounced compared to substitutions within the exoplasmic half of the TM.

Because hASBT is a sodium-dependent transporter with an apparent 2:1 Na^+/substrate stoichiometry (*9*), we next evaluated the effects of sodium withdrawal on the bile acid uptake activity of hASBT TM4 mutants. The activity of each mutant at 12 mM Na^+ (equilibrative concentration) was compared to the activity at its physiological concentration (137 mM) and normalized to the sodium sensitivity of the C270A scaffold (Figure 4). Five mutants showed significantly lower Na^+ activation ratios compared to C270A, including D163C, the only charged residue in TM4. It is interesting to note that residues D163, A171, P175, and S177 were not affected significantly by cysteine substitution at physiologic [Na^+] but revealed a significant reduction in substrate uptake at equilibrative [Na^+]. An exception is residue L172, which displayed reduced uptake rates at both sodium levels.

To determine the residues of TM4 that would likely be a part of the substrate translocation pathway, we assessed the solvent accessibility of the individual, cysteine double mutants in the presence of different MTS reagents. Only those mutants that retained significant functional activity (Figure 2) were subjected to MTS treatment. Thus, 16 active TM4 cysteine mutants were probed with 1.0 mM of the polar, membrane-impermeant MTS reagents, MTSET and MTSES (Figure 5). Residues N164, T167, S168, A171, V173, and P175 were significantly affected by co-incubation by MTS reagents and are likely participants in bile acid transport and/or modulation. As a logical next step, we probed the specificity of the observed MTS labeling and inhibition by performing the MTS incubation reaction in the presence of a natural hASBT substrate, GDCA. This would indicate whether the MTS-labeled residue lies within a functionally relevant region involved in bile acid translocation. Thus, to determine the competitive effect of the presence of bile acids on MTS inhibition, pre-equilibration with 0, 50, and 200 μM GDCA in HBSS prior to the addition of positively charged MTSET or negatively charged MTSES was carried out (Figure 6). Mutant N164C showed 40% reduction in [^{3}H]-TCA uptake in the presence of MTSES, which could not be reversed by co-incubation with GDCA. On the other hand, MTSES incubation inhibited [^{3}H]-TCA uptake of S168C to 25% of the control (absence of MTS), which was restored fully by pre-incubation with GDCA. However, this effect was not observed when S168C was incubated with positively charged MTSET; although MTSET inhibited uptake activity merely 20%, this was not ameliorated by GDCA. [^{3}H]-TCA uptake by mutant A171C was reduced to 75% of the control in the presence of MTSET, which was fully restored to control levels by the competitive protective effect of GDCA. Other mutants that were initially MTS-sensitive (i.e., T167C, V173C, and P175C; Figure 5) were not significantly protected by GDCA against MTS-induced uptake inhibition (data not shown).

To further illustrate the relative positioning of TM4 residues, we used a previously developed and validated homology model for hASBT (*11*). The SiteID program within SYBYL was used to probe solvent accessibility of the amino acid residues residing in the inner core of the protein, which can potentially play a key role in substrate translocation. Of the 10 clusters generated, clusters pertaining to TM4 had molecular volumes of 199, 57, and 12 Å^3 (clusters 2, 3, and 6) (Figure 7). Two major clusters visualized as orange (199 Å^3) and yellow (57 Å^3) predominantly line the hydrophilic face of the TM, suggestive of a highly accessible pathway. These data indicate that TM4 in combination with other TMs may play a significant role in the substrate translocation process.

DISCUSSION

Despite its critical role in bile acid and cholesterol homeostasis, the bile acid transporter hASBT has not been fully characterized at the molecular level. Hence, there is paucity of information on the specific amino acid residues that interact with substrates and cations during the translocation cycle, and a systematic approach is necessary to study the residues involved. Thus far, studies by our laboratory and others have suggested an intricate role for various charged residues in substrate and sodium ion interaction (*11, 27–29*). Furthermore, we have reported that TM6 promotes helical flexibility, owing to the presence of Pro and Gly residues (*30*), whereas TM7 plays a structural role in substrate translocation (*31*). Recent studies on extracellular loop 3 (*28*), which interconnects TM6 and TM7, found that this protein segment contains sodium-sensing residues in addition to substrate interaction sites. The present study provides compelling evidence in support of the functional relevance of TM4 in the uptake of bile acids by hASBT; furthermore, TM4 may partly line the substrate permeation pathway.

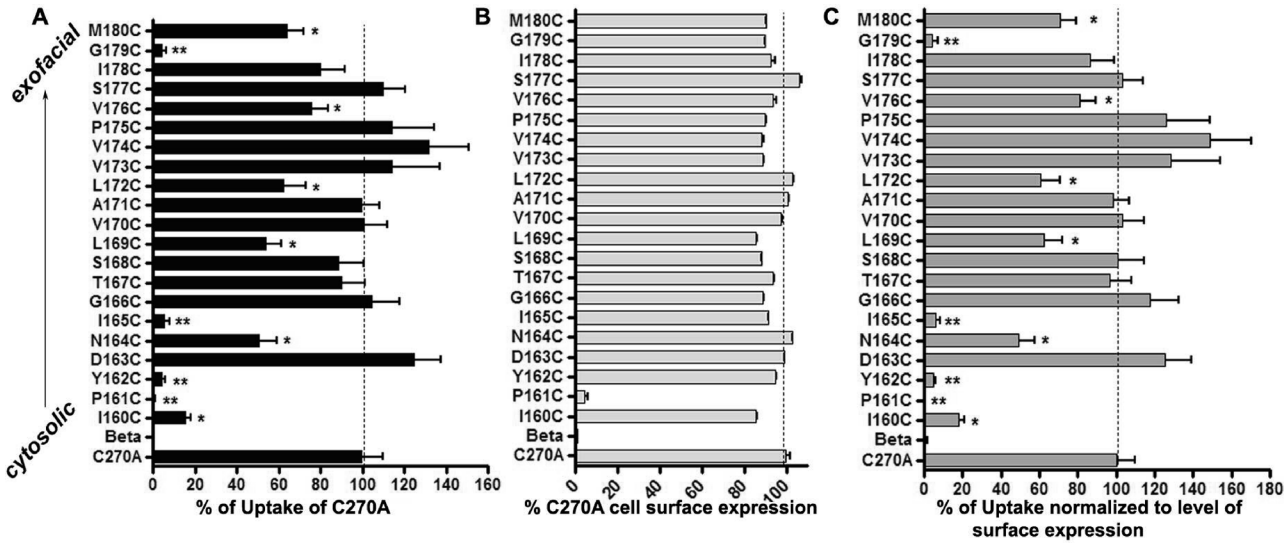

FIGURE 3: Uptake activity of TM4 mutants of C270A−hASBT in COS-1 cells. (A) Uptake was carried out at 5 μM [^{3}H]-TCA. Results are given as a percentage of the mutant uptake relative to C270A. Each bar is the mean ± standard error (SE) ($n = 3$). (B) Averaged densitometry analysis of the surface expression of the cysteine mutants normalized to the internal marker α-integrin and represented as a percentage of C270A expression. (C) [^{3}H]-TCA uptake activity after normalization for the average hASBT cell membrane expression. An asterisk (∗) denotes statistical significance ($p < 0.05$).

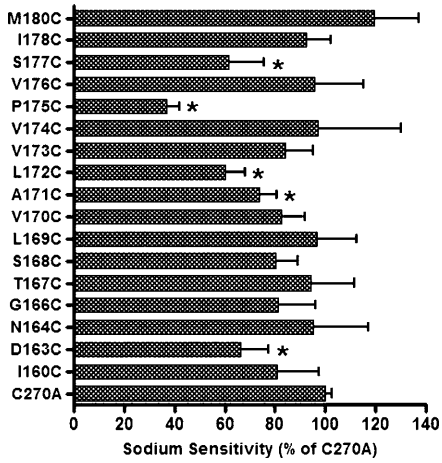

FIGURE 4: Sodium activation studies of functionally active single-C C270A mutants. COS-1 cells transfected with TM4 Cys mutants were incubated in uptake medium (5 μM [^{3}H]-TCA) containing a low (12 mM) and saturated (137 mM) sodium concentration for 12 min at 37 °C. Each bar represents the sodium sensitivity compare to that of C270A and is represented as mean ± SE ($n = 3$). An asterisk (∗) represents significantly different observations ($p < 0.05$).

To identify residues responsible for bile acid and/or Na^+ interaction within TM4, we performed systematic mutagenesis of all 21 residues spanning this transmembrane region. Each individual amino acid residue was mutated to Cys, using the relatively MTS-insensitive C270A scaffold (*27*), followed by SCAM analysis. All TM4 C270A double mutants were expressed at the plasma membrane, except P161C. All functionally inactive mutants (Figure 2) resulting from Cys substitution were evolutionarily conserved (Figure 1B), suggesting their critical role in ASBT function.

Uptake of the prototypical substrate for hASBT, TCA, was significantly reduced for 9 of 21 Cys mutants (not including P161C). Interestingly, the majority of the affected mutants fall within the cytoplasmic half of the transmembrane segment (amino acids 160–165), and these residues are affected to a greater extent than the residues closer to the exofacial half of the TM (Figure 3). Amino acid position 167 is poorly conserved across species, containing either a Thr or Ile residue (Figure 1B). Our data indicate that Cys replacement is also well-tolerated, suggesting that this position and perhaps its neighboring residues do not fulfill a critical role in hASBT function. Helical wheel analysis of TM4 indicates that residues significantly affected by mutation alone occupy one distinct "face" of the α-helical TM projection predicted by computational methods (Figure 7A). Furthermore, this face is predicted to be adjacent to at least two solvent-accessible pockets, which are positioned between transmembrane domains 3, 4, and 5 (Figure 7B). Importantly, the largest solvent-accessible pocket lines the cytosolic half of TM4, which is in agreement with our experimental data and suggests significant solvent accessibility of the cytosolic region.

Interestingly, the substitution of proline residues with cysteine at two different locations within TM4 resulted in contrasting effects on substrate uptake. Whereas the uptake of taurocholate by the P175C mutant was not significantly affected (Figure 2), P161C failed to express at the plasma membrane, suggesting its putative role in protein structure, folding, or stability. A possible explanation for the divergent roles of Pro residues in TM4 may be attributed to their relative localization within the transmembrane helix. Protein structural studies have shown that, at the extremes of the transmembrane region, proline residues may induce helical termination or initiation, whereas proline residues located centrally within TM segments could introduce a kink or bend, whose degree is influenced by the surrounding tertiary protein structure (*32–34*). Therefore, P161 may be critical for helix termination or initiation, whereas P175 may form a kink in the transmembrane segment; however, the absence of such a kink may not significantly alter substrate access and/or handling by the transporter protein. Interestingly, both proline residues line the same face in the putative α-helical arrangement of TM4 (Figure 7A) along with the only functionally inactive residues Y162, I165, and G179.

Because of the essential role of Na^+ as a cosubstrate for

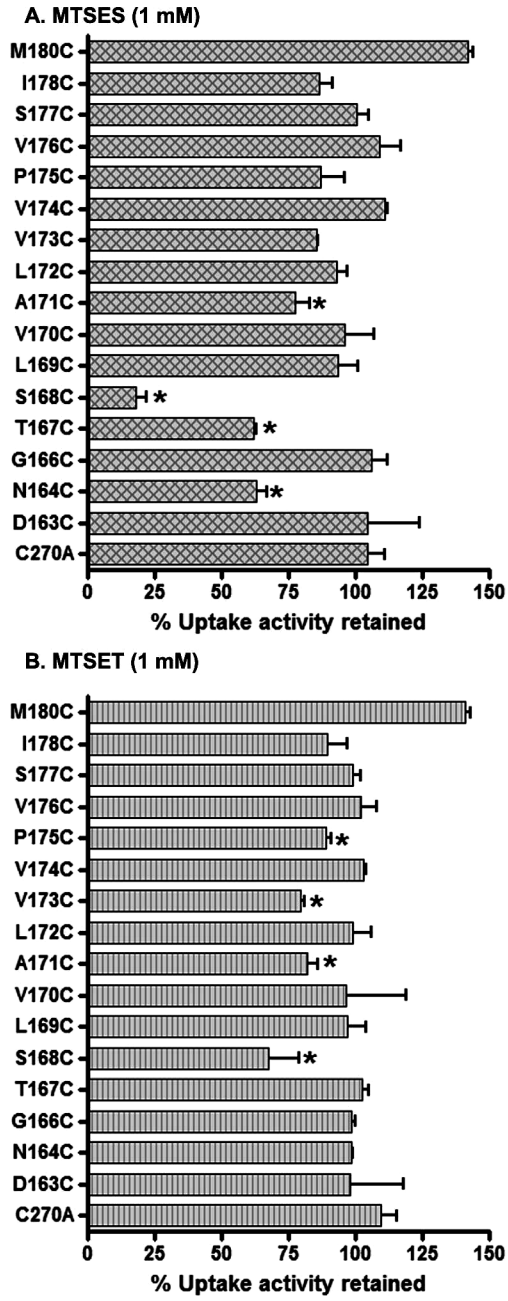

FIGURE 5: Effect of MTS reagents on [^{3}H]-TCA uptake activities of the TM4 cysteine-scanning mutants. At 48–72 h post-transfection, COS-1 cells expressing Cys mutants were treated with (A) 1.0 mM MTSES or (B) 1.0 mM MTSET for 10 min at room temperature. Cells were washed and incubated in uptake medium containing 5 μM [^{3}H]-TCA for 12 min at 37 °C. Individual controls for each mutant were treated with uptake buffer. Results represent the percentage of TCA uptake activity retained. Each bar is the mean $\pm$ SE ($n = 3$). An asterisk (*) indicates values significantly different from individual controls ($p \leq 0.05$).

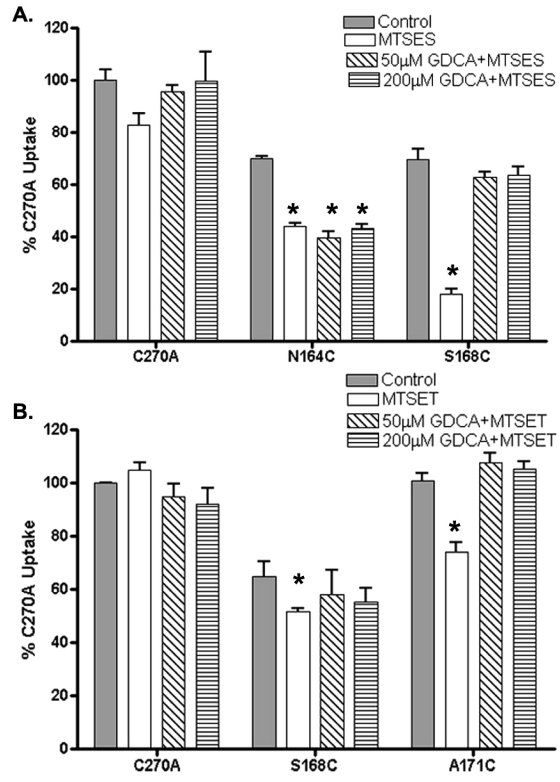

FIGURE 6: Effect of GDCA on the affinity of (A) MTSES or (B) MTSET for TM4 cysteine mutants. COS-1 cells transfected with hASBT, C270A, and the TM4 cysteine mutants were pre-incubated for 3 min with GDCA (up to 200 μM) prior to 5 min of incubation with 1.0 mM MTSES or MTSET at room temperature. The cells were washed twice and equilibrated in uptake buffer for 15 min. [^{3}H]-TCA (5.0 μM) uptake was measured at 37 °C for 12 min. Control wells with no MTS or no GDCA were treated similarly. Each bar is displayed as a percentage of the C270A control (no MTS reagent), and each bar is the mean $\pm$ SE ($n = 3$).

hASBT function, we sought to determine the effects of mutation at physiological and equilibrative sodium concentrations. We identified five residues (D163, A171, L172, P175, and S177) that were affected in their ability to transport taurocholate at low sodium concentration (Figure 4). Not surprisingly, D163, the only negatively charged residue within TM4 was affected by a decrease in positive-ion concentration. Overall, the observed effects may be attributed to conformational changes brought about by the residues to form or maintain structures involved in Na^+ interaction. However, the effects of an altered sodium concentration is minimal, and therefore, the effects are likely indirect in nature. On the basis of our present data, we propose that there is no direct role for Na^+ interaction with TM4.

To further probe the predicted solvent accessibility of the respective hASBT mutants, we performed SCAM analysis by incubating each individual Cys mutant with membrane-impermeable MTS reagents prior to performing uptake studies. Visualization of the MTS inhibition data on a helical wheel projection of TM4 (Figure 7A) demonstrates that five of six MTS-accessible residues are clustered together along one face of a putative TM4 α helix. Our previous SCAM studies with TM6 and TM7 revealed that the exofacial side was predominantly solvent-accessible (*30, 31*). However, contrary to expectations, amino acid residues within the cytosolic to middle regions of TM4 were highly affected upon MTS exposure (Figure 5). This would suggest that the substrate permeation pathway is either tortuous or that helical tilt of individual transmembrane domains is a contributing factor to forming a substrate-accessible pore. Our results further demonstrate that a positive charge introduced as a result of MTSET incubation was better tolerated than the addition of a negative charge by the MTSES reagent (Figure 5), suggesting that TM4 favors a electropositive environment, which may be required for the interaction with negatively charged moieties on natural bile acid analogues. Although MTSES and MTSET modified the protein with opposite

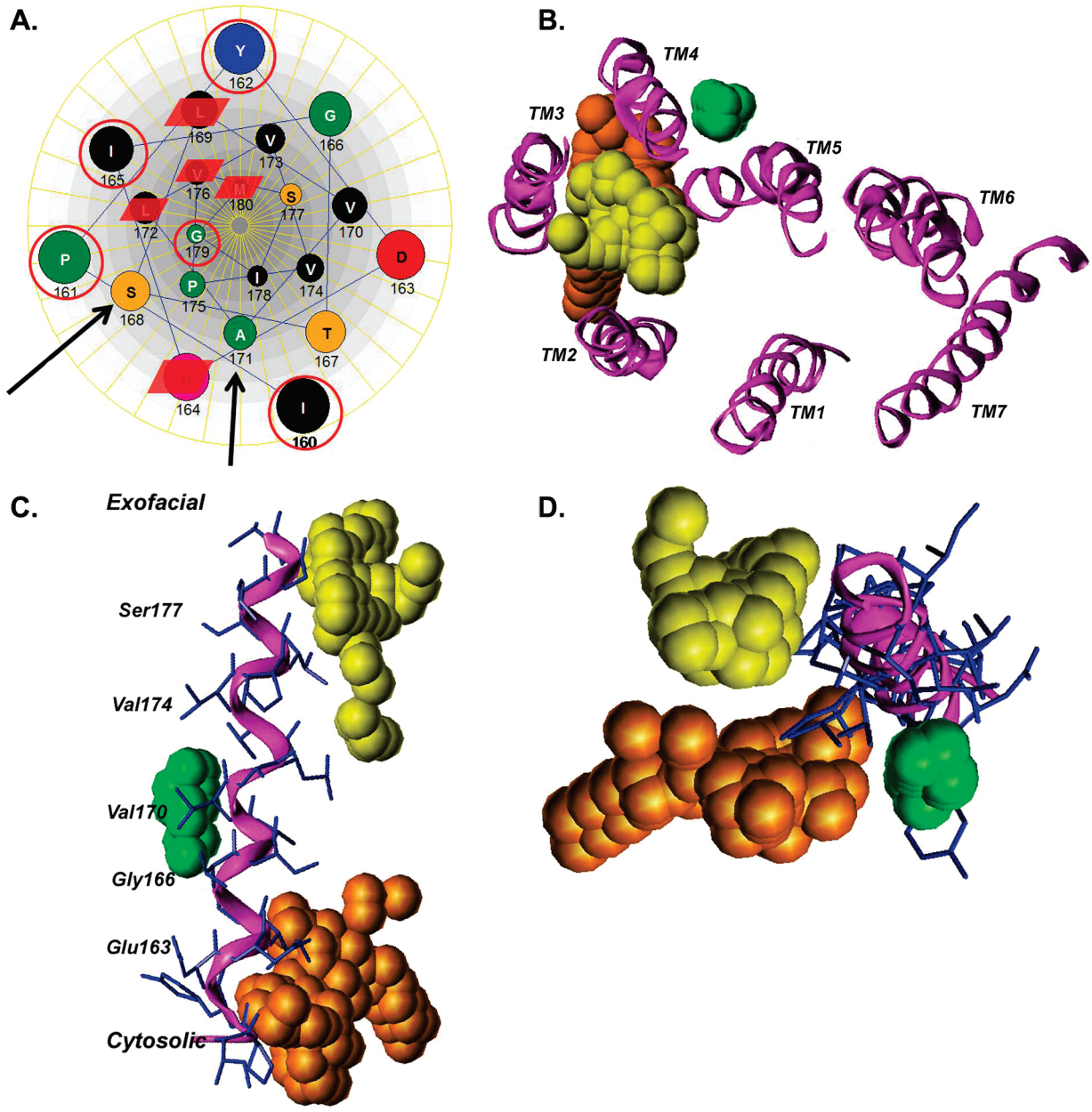

FIGURE 7: Computational analysis of hASBT. (A) Helical wheel representation of TM4 of hASBT visualized from the cytoplasmic side of the TM4. Amino acids are represented by the standard single-letter code. Red open circles indicate residues showing ≤20% uptake, and highlighted are the residues that show moderate reduction in TCA uptake upon cysteine substitution. Black arrows indicate solvent-accessible residues. (B) Solvent-accessibility analysis of hASBT exofacial view. The grid method within SiteID was used to determine accessible regions of a previously developed homology model of the hASBT. Major clusters are visualized by a colored sphere, and for clarity, only clusters surrounding TM4 were visualized. The resulting yellow, orange, and green with molecular volumes of 57, 199, and 12 Å^3 (clusters 3, 2, and 6) occupy domains spatially favorable to the formation of hydrogen bonds with TM4 amino acids. Amino acid side chains have been omitted for clarity. (C) Side view of the predicted three-dimensional α-helical arrangement of TM4 residues along its vertical axis. Top is the exofacial side, and the side chains are shown without hydrogen atoms for clarity. (D) Top view of the arrangement shown in C from the exofacial side.

charges, they affected S168C to a similar extent, suggesting that modification at this position is independent of the electrostatic environment. An apparent lack of inhibition for the solvent-accessible cytosolic half by MTSET but not MTSES may indicate size-restricted access, which could be attributed to the differences in molecular volume of MTSET (~109 Å^3) versus MTSES (~90 Å^3).

Another mutant that demonstrated significant inhibition only by MTSES is N164C (Figure 5), which is situated close to the transmembrane−cytosolic interface; furthermore, its inactivation by MTSES could not be ameliorated by co-incubation with GDCA (Figure 6). Whereas we cannot exclude the possibility that a small fraction of MTSES may permeate the lipid bilayer, we believe it is unlikely that N164C inactivation occurs via cytosolic access to this residue for the following reasons: (1) the residues adjacent to N164, i.e., G166 and D163, are not affected by either MTS reagent; (2) permeation of MTSES, which bears a negative charge at physiological pH, across the lipid bilayer is presumably low, whereas the fraction that may eventually reach the cytosol would immediately react with abundantly present cytosolic proteins. Therefore, we speculate that access to N164C by MTSES may occur via a small solvent pocket accessible only to this relatively small MTS reagent (M_w ~ 220 Da). This

pocket, which may lie adjacent to or in contact with the substrate permeation pathway would not be accessible to the relatively larger natural substrate, GDCA ($M_w \sim 468$ Da), resulting in the observed lack of substrate protection.

MTS incubation studies in the presence of the natural bile acid analogue, GDCA, were performed to determine whether MTS modification occurs at amino acid residues directly interacting with substrate (Figure 6). Hallén and colleagues (*27*) previously demonstrated protection of wt-hASBT from inactivation by MTSET (1 mM, 20% of control) by pretreatment with 50 or 200 μM GDCA (to 60 and 80% of control values, respectively). Interestingly, while we demonstrate substrate protection for mutants S168C and A171C, we do not observe a strict concentration-dependent restoration of hASBT function in the presence of GDCA. We have previously demonstrated that MTS sensitivity of wt-hASBT is primarily due to inactivation of Cys270 (*31*), a highly accessible cysteine residue, which lies in close proximity to sodium and substrate interaction sites. Because the C270A mutant scaffold is mostly insensitive to MTS treatment, we do not expect to see a linear correlation between substrate protection and GDCA concentration based on limited accessibility of residues that lie deep within the permeation pathway. Considering that uptake activities of S168C and A171C were at least partially restored in the presence of GDCA, we posit that GDCA and MTS reagents access the same solvent pocket within hASBT protein. Even though mutation of S168 and A171 to cysteine did not affect uptake activity (Figure 3), they appear to form part of the substrate translocation pathway. Their relative importance becomes obvious when visualizing the respective positions of S168 and A171 on a helical wheel projection of TM4 (Figure 7A), namely, occupation of the same helical face as the loss-of-function mutants I165C and G179C. This striking conservation of α-helical periodicity provides further credence to our proposed model for TM4 and hASBT.

Previous genotyping studies to determine potential polymorphisms responsible for PBAM syndrome, identified a phenotypically silent A/S171 point mutation with a 28% allele frequency among control subjects (*25*). Incidentally, this otherwise common polymorphism is only present in the wild-type *Danio rerio* (zebrafish) asbt sequence (Figure 1B). As expected, substitution of A171 with Cys, a small, polar residue with physicochemical characteristics comparable to Ser, did not significantly alter its function (Figure 3). However, we found that A171C was moderately affected (~80% uptake versus the control) by MTS reagents (Figure 5), indicating high solvent accessibility at this residue; this was further supported by full restoration of uptake activity when the MTS reagent was co-incubated with the natural ligand GDCA (Figure 6). Additionally, we determined moderate sodium sensitivity for this residue, reaffirming its importance in substrate translocation. Combined, we hypothesize that A171 may interact with the substrate and could constitute part of the ligand translocation pathway.

In summary, our data suggest that TM4 has a distinct helical face that contains residues critical for transport function and conformational stability. Contrary to expectations, we found that TM4 solvent accessibility was conserved to the middle to cytoplasmic region rather than the exoplasmic half. TM4 contains two Pro residues that were assigned divergent functions; whereas P175 may play a role in helical twisting, P161 is critical for protein stability and folding. Although hASBT is a sodium-dependent solute transporter, TM4 does not appear to play a direct role in ion cotransport. In combination with our previous studies, our present results provide further insight into understanding the molecular mechanisms underlying structure and function of hASBT. These studies may enable strategies for rational drug design aimed at inhibiting intestinal bile acid reabsorption and/or cholesterol-lowering therapy.

ACKNOWLEDGMENT

The authors thank Dr. Akash Khandelwal for his assistance with the computational aspects of this study.

REFERENCES

1. Dawson, P. A., and Oelkers, P. (1995) Bile acid transporters. *Curr. Opin. Lipidol. 6*, 109–114.
2. Alpini, G., Ulrich, C., Roberts, S., Phillips, J. O., Ueno, Y., Podila, P. V., Colegio, O., LeSage, G. D., Miller, L. J., and LaRusso, N. F. (1997) Molecular and functional heterogeneity of cholangiocytes from rat liver after bile duct ligation. *Am. J. Physiol. 272*, G289–G297.
3. Lazaridis, K. N., Pham, L., Tietz, P., Marinelli, R. A., deGroen, P. C., Levine, S., Dawson, P. A., and LaRusso, N. F. (1997) Rat cholangiocytes absorb bile acids at their apical domain via the ileal sodium-dependent bile acid transporter. *J. Clin. Invest. 100*, 2714–2721.
4. Hagenbuch, B., Lubbert, H., Stieger, B., and Meier, P. J. (1990) Expression of the hepatocyte Na^+/bile acid cotransporter in *Xenopus laevis* oocytes. *J. Biol. Chem. 265*, 5357–5360.
5. Hagenbuch, B., Stieger, B., Foguet, M., Lubbert, H., and Meier, P. J. (1991) Functional expression cloning and characterization of the hepatocyte Na^+/bile acid cotransport system. *Proc. Natl. Acad. Sci. U.S.A. 88*, 10629–10633.
6. Wong, M. H., Oelkers, P., and Dawson, P. A. (1995) Identification of a mutation in the ileal sodium-dependent bile acid transporter gene that abolishes transport activity. *J. Biol. Chem. 270*, 27228–27234.
7. Wong, M. H., Oelkers, P., Craddock, A. L., and Dawson, P. A. (1994) Expression cloning and characterization of the hamster ileal sodium-dependent bile acid transporter. *J. Biol. Chem. 269*, 1340–1347.
8. Lazaridis, K. N., Tietz, P., Wu, T., Kip, S., Dawson, P. A., and LaRusso, N. F. (2000) Alternative splicing of the rat sodium/bile acid transporter changes its cellular localization and transport properties. *Proc. Natl. Acad. Sci. U.S.A. 97*, 11092–11097.
9. Weinman, S. A., Carruth, M. W., and Dawson, P. A. (1998) Bile acid uptake via the human apical sodium−bile acid cotransporter is electrogenic. *J. Biol. Chem. 273*, 34691–34695.
10. Banerjee, A., and Swaan, P. W. (2006) Membrane topology of human ASBT (SLC10A2) determined by dual label epitope insertion scanning mutagenesis. New evidence for seven transmembrane domains. *Biochemistry 45*, 943–953.
11. Zhang, E. Y., Phelps, M. A., Banerjee, A., Khantwal, C. M., Chang, C., Helsper, F., and Swaan, P. W. (2004) Topology scanning and putative three-dimensional structure of the extracellular binding domains of the apical sodium-dependent bile acid transporter (SLC10A2). *Biochemistry 43*, 11380–11392.
12. Shih, D. Q., Bussen, M., Sehayek, E., Ananthanarayanan, M., Shneider, B. L., Suchy, F. J., Shefer, S., Bollileni, J. S., Gonzalez, F. J., Breslow, J. L., and Stoffel, M. (2001) Hepatocyte nuclear factor-1α is an essential regulator of bile acid and plasma cholesterol metabolism. *Nat. Genet. 27*, 375–382.
13. Chen, F., Ma, L., Dawson, P. A., Sinal, C. J., Sehayek, E., Gonzalez, F. J., Breslow, J., Ananthanarayanan, M., and Shneider, B. L. (2003) Liver receptor homologue-1 mediates species- and cell line-specific bile acid-dependent negative feedback regulation of the apical sodium-dependent bile acid transporter. *J. Biol. Chem. 278*, 19909–19916.
14. Neimark, E., Chen, F., Li, X., and Shneider, B. L. (2004) Bile acid-induced negative feedback regulation of the human ileal bile acid transporter. *Hepatology 40*, 149–156.

15. Root, C., Smith, C. D., Winegar, D. A., Brieaddy, L. E., and Lewis, M. C. (1995) Inhibition of ileal sodium-dependent bile acid transport by 2164U90. *J. Lipid Res. 36*, 1106–1115.
16. Chiang, J. Y., Kimmel, R., Weinberger, C., and Stroup, D. (2000) Farnesoid X receptor responds to bile acids and represses cholesterol 7α-hydroxylase gene (CYP7A1) transcription. *J. Biol. Chem. 275*, 10918–10924.
17. Higaki, J., Hara, S., Takasu, N., Tonda, K., Miyata, K., Shike, T., Nagata, K., and Mizui, T. (1998) Inhibition of ileal Na^+/bile acid cotransporter by S-8921 reduces serum cholesterol and prevents atherosclerosis in rabbits. *Arterioscler., Thromb., Vasc. Biol. 18*, 1304–1311.
18. West, K. L., Zern, T. L., Butteiger, D. N., Keller, B. T., and Fernandez, M. L. (2003) SC-435, an ileal apical sodium co-dependent bile acid transporter (ASBT) inhibitor lowers plasma cholesterol and reduces atherosclerosis in guinea pigs. *Atherosclerosis 171*, 201–210.
19. Tremont, S. J., Lee, L. F., Huang, H. C., Keller, B. T., Banerjee, S. C., Both, S. R., Carpenter, A. J., Wang, C. C., Garland, D. J., Huang, W., Jones, C., Koeller, K. J., Kolodziej, S. A., Li, J., Manning, R. E., Mahoney, M. W., Miller, R. E., Mischke, D. A., Rath, N. P., Fletcher, T., Reinhard, E. J., Tollefson, M. B., Vernier, W. F., Wagner, G. M., Rapp, S. R., Beaudry, J., Glenn, K., Regina, K., Schuh, J. R., Smith, M. E., Trivedi, J. S., and Reitz, D. B. (2005) Discovery of potent, nonsystemic apical sodium-codependent bile acid transporter inhibitors (part 1). *J. Med. Chem. 48*, 5837–5852.
20. Huang, H. C., Tremont, S. J., Lee, L. F., Keller, B. T., Carpenter, A. J., Wang, C. C., Banerjee, S. C., Both, S. R., Fletcher, T., Garland, D. J., Huang, W., Jones, C., Koeller, K. J., Kolodziej, S. A., Li, J., Manning, R. E., Mahoney, M. W., Miller, R. E., Mischke, D. A., Rath, N. P., Reinhard, E. J., Tollefson, M. B., Vernier, W. F., Wagner, G. M., Rapp, S. R., Beaudry, J., Glenn, K., Regina, K., Schuh, J. R., Smith, M. E., Trivedi, J. S., and Reitz, D. B. (2005) Discovery of potent, nonsystemic apical sodium-codependent bile acid transporter inhibitors (part 2). *J. Med. Chem. 48*, 5853–5868.
21. Swaan, P. W., Hillgren, K. M., Szoka, F. C., Jr., and Oie, S. (1997) Enhanced transepithelial transport of peptides by conjugation to cholic acid. *Bioconjugate Chem. 8*, 520–525.
22. Tolle-Sander, S., Lentz, K. A., Maeda, D. Y., Coop, A., and Polli, J. E. (2004) Increased acyclovir oral bioavailability via a bile acid conjugate. *Mol. Pharm. 1*, 40–48.
23. Hussainzada, N., Banerjee, A., and Swaan, P. W. (2006) Transmembrane domain VII of the human apical sodium-dependent bile acid transporter ASBT (SLC10A2) lines the substrate translocation pathway. *Mol. Pharmacol. 70*, 1565–1574.
24. Hallen, S., Mareninova, O., Branden, M., and Sachs, G. (2002) Organization of the membrane domain of the human liver sodium/bile acid cotransporter. *Biochemistry 41*, 7253–7266.
25. Oelkers, P., Kirby, L. C., Heubi, J. E., and Dawson, P. A. (1997) Primary bile acid malabsorption caused by mutations in the ileal sodium-dependent bile acid transporter gene (SLC10A2). *J. Clin. Invest. 99*, 1880–1887.
26. Banerjee, A., Ray, A., Chang, C., and Swaan, P. W. (2005) Site-directed mutagenesis and use of bile acid−MTS conjugates to probe the role of cysteines in the human apical sodium-dependent bile acid transporter (SLC10A2). *Biochemistry 44*, 8908–8917.
27. Hallen, S., Fryklund, J., and Sachs, G. (2000) Inhibition of the human sodium/bile acid cotransporters by side-specific methanethiosulfonate sulfhydryl reagents: Substrate-controlled accessibility of site of inactivation. *Biochemistry 39*, 6743–6750.
28. Banerjee, A., Hussainzada, N., Khandewal, A., and Swaan, P. W. (2007) Electrostatic and potential cation−π forces guide interaction of extracellular loop III in human apical sodium-dependent bile acid transporter (hASBT) with Na^+ and bile acids. *Biochem. J.*
29. Sun, A. Q., Balasubramaniyan, N., Chen, H., Shahid, M., and Suchy, F. J. (2006) Identification of functionally relevant residues of the rat ileal apical sodium-dependent bile acid cotransporter. *J. Biol. Chem. 281*, 16410–16418.
30. Hussainzada, N., Khandewal, A., and Swaan, P. W. (2008) Conformational flexibility of helix VI is essential for substrate permeation of the human apical sodium-dependent bile acid transporter (ASBT). *Mol. Pharmacol. 73*, 305–313.
31. Hussainzada, N., Banerjee, A., and Swaan, P. W. (2006) Transmembrane domain VII of the human apical sodium-dependent bile acid transporter ASBT (SLC10A2) lines the substrate translocation pathway. *Mol. Pharmacol. 70*, 1565–1574.
32. Ceruso, M. A., and Weinstein, H. (2002) Structural mimicry of proline kinks: Tertiary packing interactions support local structural distortions. *J. Mol. Biol. 318*, 1237–1249.
33. Hassan, K. A., Galea, M., Wu, J., Mitchell, B. A., Skurray, R. A., and Brown, M. H. (2006) Functional effects of intramembranous proline substitutions in the staphylococcal multidrug transporter QacA. *FEMS Microbiol. Lett. 263*, 76–85.
34. Cordes, F. S., Bright, J. N., and Sansom, M. S. (2002) Proline-induced distortions of transmembrane helices. *J. Mol. Biol. 323*, 951–960.

BI702498W